CHILEAN JOURNAL of AGRICULTURAL RESEARCH

CHILEANJAR
CHILEAN JOURNAL of AGRICULTURAL RESEARCH

RESEARCH ARTICLE

Potential of infrared radiation-thermography for screening salt-tolerant 'Pokkali' rice seedlings

Chonticha Phromduang[1], Nantawan Kanawapee[2], Piyada Theerakulpisut[1], and Watanachai Lontom[1*]

[1]Khon Kaen University, Faculty of Science, Department of Biology, Khon Kaen 40002, Thailand.
[2]Nakhon Phanom University, Faculty of Science, Nakhon Phanom 48000, Thailand.
[*]Corresponding author (watalo@kku.ac.th).
Received: 16 September 2023; Accepted: 8 November 2023, doi:10.4067/S0718-58392024000100110

ABSTRACT

Screening for salt-tolerance plants has been carried out to enhance yield production. Consequently, the physiological and growth parameters were performed. These methods are labor-intensive and destructive. Nowadays, non-destructive thermography has been used for detecting infrared radiation under water stress. However, monitoring progressive leaf temperature under salt stress conditions has rarely been reported in rice (*Oryza sativa* L.) This study aims to monitor salt stress response in 'Pokkali' rice seedlings using infrared radiation (IR) thermography together with physiological and growth parameters. Twenty-six-day-old 'Pokkali' rice seedlings, standard salt tolerant, were subjected to 80, 120, and 160 mM NaCl for 8 d under hydroponic conditions. Our study found that NaCl condition influences the emission of infrared radiation and the elevation in leaf temperature. Notably, seedlings exposed to 160 mM NaCl after 8 d exhibited significantly higher temperature changes (5.21 °C), and higher crop water stress index (CWSI). Likewise, we observed lower reductions in transpiration rate (88.19%), stomatal conductance (92.78%), and photosynthetic rate (70.99%). Together, the correlation matrix revealed a strong relationship between CWSI and leaf gas exchange parameters, including photosynthetic rate, transpiration rate, and stomatal conductance. Additionally, IR-thermal indices and some physiological parameters contributed to the segregation between control and salt stress groups. Therefore, the simple thermal imaging technique can effectively monitor salt stress responses at various NaCl concentrations in the 'Pokkali' rice. The application of IR-thermography will be applied to various abiotic stressors and different rice cultivars in the future.

Key words: *Oryza sativa*, 'Pokkali' rice, salt stress, salt tolerance, screening, thermal imaging.

INTRODUCTION

Infrared radiation (IR)-thermography is a non-destructive method for detecting infrared radiation emissions. Infrared radiation is emitted from objects with wavelengths estimated between 700 nm and 1000 µm (Tsai and Hamblin, 2017). Nowadays, IR technology has been utilized for detecting leaf temperature under plant water stress such as drought and salinity stress. Importantly, salinity stress is a main challenge worldwide where combined salt-affected area amounts to more than 800 million hectares (FAO, 2022). This major challenge eventually causes a decrease in crop production (Munns and Tester, 2008). An advanced approach to enhance crop yield and productivity under unfavorable conditions is through the screening of salt-tolerant plants. Screening for salt-tolerance has been investigated via the parameters which are related to plant water stress, photosynthesis, and growth performances such as electrolyte leakage (EL), malondialdehyde (MDA) content, and relative water content (RWC). However, these methods are destructive and laborious. To overcome the obstacles, IR-thermography is the best alternative way with their special properties which are non-destructive (Sirault et al., 2009; Bayoumi et al., 2014; Orzechowska et al., 2021) and simple technique.

The IR-thermography has been documented as an effective method for screening salt tolerance in cereal crops. The previous study of Sirault et al. (2009) demonstrates the capability of IR thermal imaging to assess a wide range of wheat genotypes with diverse stomatal traits, particularly those associated with salt tolerance. Together, the different salt stress responses between NaCl concentration in barley, the most tolerant in cereal crop (Munns and Tester, 2008), were detected with IR emission from their leaf temperature via ThermaCAM SC660 IR camera (FLIR Systems Inc., Wilsonville, Oregon, USA). In their study, James and Sirault (2012) explored the phenotyping of salinity tolerance in wheat seedlings using a Matlab program to automatically process IR-thermal images. Remarkably, this method demonstrated a clear ability to distinguish between control and 100 mM NaCl-treated seedlings. Also, Siddiqui et al. (2014) found a strong relationship among stomatal conductance, the relative water stress, and IR thermal images in rice (*Oryza sativa* L. 'Donggin') under salinity conditions. Simultaneously, Bayoumi et al. (2014) demonstrated a significant correlation between thermal indices, namely crop water stress index (CWSI) and index of stomatal conductance (I_G), and the K^+/Na^+ ratio in 10 bread wheat genotypes. Notably. The CWSI and stomatal conductance showed a strong relationship. Additionally, the thermal index was applied for predicting maize yield (Pradawet et al., 2022). In this regard, it is clear that IR-thermography can screen salt-tolerant crop plants and correlate with stomatal conductance. However, the monitoring of leaf temperature due to salt stress has not been examined together with some physiological performance and growth performance. Also, the monitoring of IR-thermography under different NaCl concentrations have not been investigated. Apart from that, 'Pokkali' rice, known for its standard salt tolerance (Chen et al., 2019; Mishra et al., 2021), serves as an exemplary model for monitoring a wide range of NaCl concentrations.

The objective of this research was to monitor changes in leaf temperature, CWSI, and I_G with IR thermography together with studying the physiological responses under different salt stress conditions in 'Pokkali' rice seedlings. The result can be utilized to apply IR-thermography in various unfavorable stress and various rice cultivars/lines in future research.

MATERIALS AND METHODS

Plant material and growing conditions

The experiment was laid out as a completely randomized design with four replicates. 'Pokkali' rice (*Oryza sativa* L.) seedlings were grown in a greenhouse from December 2021 to February 2022 at the Department of Biology, Khon Kean University, Khon Kean, Thailand. 'Pokkali' rice seeds were obtained from the Salt-tolerant Rice Research Group, Faculty of Science, Khon Kaen University. 'Pokkali' seeds were sterilized with 5% v/v sodium hypochlorite for 15 min, then cleaned with distilled water five times. The seeds were soaked in distilled water for 1 d and then were incubated on filter paper soaked with distilled water, which was placed in petri dishes, for 4 d under room temperature conditions. After that, four germinated seeds were transplanted into the floating Styrofoam on the pot which was filled with 3 L chlorine-evaporated tap water for 4 d. The tap water was then replaced with half-strength Yoshida solution (Yoshida et al., 1976) for 7 d followed by full-strength Yoshida solution until the seedlings were 26 d old during which the solutions were renewed every 5 d. Seedlings were subjected to four treatments: 1) Control group grown in Yoshida solution without NaCl added throughout the experiment, 2) 80 mM NaCl, 3) 120 mM, and 4) 160 mM NaCl. The salt stress treatments, including treatments 2, 3, and 4, were started by adding 40 mM NaCl to the full-strength Yoshida solution for 3 d. Then, seedlings in treatments 2, 3, and 4 received 80, 120, and 160 mM NaCl for 5 d, respectively. After that, infrared radiation (IR) thermal images of seedlings were taken, and seedlings were harvested to measure growth and physiological parameters.

IR thermography

The IR thermal images were captured using the FLIR C2 camera (FLIR Systems, Inc., Wilsonville, Oregon, USA). Each image was composed of artificial references and seedlings in the control group juxtaposed with salt-treated seedlings in 80, 120, and 160 mM NaCl treatments. The pictures were taken from 10:00 to 12:30 h

beginning 1 d before exposure to salt stress (day 0) until the last day of salt stress condition (8 d after stress [DAS]). To maximize the plant-to-background temperature contrast, brown acrylic sheets were used as a background in this experiment. The dry green cotton fabric was used as a dry artificial reference, while the completely wet fabric represented a wet artificial reference. After that, thermal images were analyzed using the line measurement function in FLIR Tools software (Teledyne FLIR LLC, Wilsonville, Oregon, USA). Average temperatures of 10 lines that were dragged across artificial references, canopy or uppermost leaf areas in each picture were recorded, and used to calculate crop water stress index (CWSI) and index of stomatal conductance (I_G) as in the Equations 1 and 2, respectively (Jones, 1999):

$$CWSI = (T_{canopy} - T_{wet})/(T_{dry} - T_{wet}) \quad (1)$$

$$I_G = (T_{dry} - T_{leaf})/(T_{leaf} - T_{wet}) \quad (2)$$

where T_{canopy} is canopy temperature, T_{leaf} is leaf temperature, T_{wet} is wet reference temperature, and T_{dry} is dry reference temperature.

Plant growth measurements

The rice seedlings were sampled with one plant per replicate and then washed with water, dried with tissue paper, and arranged on the flute board background. After that, the seedlings were taken a photo which was positioned from the top view of the background. These photos were used to measure shoot length and root length using ImageJ software (National Institutes of Health, Bethesda, Maryland, USA). After that, plant roots and stems were separated and weighed with analytical balance for fresh weight (FW). Samples were oven-dried at 80 °C for 3 d and weighed again for dry weight (DW).

Physiological measurements

Relative water content. Two mid-leaf sections with 2 cm length each were cut from the first fully expanded leaf and immediately weighed using analytical balance for FW measurement. The leaf samples were then submerged in a plastic petri dish containing deionized water for 8 h. The turgid weight (TW) of the samples was measured right after they were blotted with tissue paper. Subsequently, the leaf samples were oven-dried at 80 °C for 48 h and weighed for DW measurement. Relative water content (RWC) was computed as follows (Weatherly, 1951):

$$RWC\ (\%) = [(FW - DW)/(TW - DW)] \times 100$$

Malondialdehyde content. Approximately 0.2 g leaf tissue was finely ground with 1 mL 0.1% (w/v) trichloroacetic acid (TCA) and then centrifuged at 15000 rpm for 10 min at 4 °C. The 0.5 mL aliquot of the supernatant was mixed with 1.5 mL 0.5% thiobarbituric acid (TBA) in 20% (w/v) TCA solution. The mixture was incubated in a water bath at 95 °C for 25 min. The reaction was stopped by soaking the tube in an ice box. The absorbances of the mixture were measured at 532 and 600 nm using a spectrophotometer. Malondialdehyde (MDA) content was calculated using the formula proposed by Heath and Packer (1968):

$$MDA\ (mM) = (A_{532} - A_{600})/155$$

where 155 is the molar extinction coefficient ($mM^{-1}\ cm^{-1}$) at 532 nm.

Electrolyte leakage. A 0.1 g leaf sample was cut into equal-sized pieces and placed in a centrifuge tube with 10 mL deionized water, and then incubated for 24 h under room temperature. After that, the electrical conductivity (EC1) was measured using an EC meter (PL-700PCS GOnDO, Taipei City, Taiwan). The tube was placed in a 100 °C water bath for 25 min and cooled at room temperature. The EC2 was then measured. Electrolyte leakage (EL) was calculated according to Filek et al. (2012):

$$EL\ (\%) = (EC1/EC2) \times 100$$

Leaf gas exchange. Photosynthesis rate (P_n), stomatal conductance (g_s), and transpiration rate (T_r) were assessed using portable gas exchange analyzer LI-6400-XT (6400-02B Red/Blue LightSource, LI-COR Inc., Lincoln, Nebraska, USA). The measurements were taken on the second fully expanded leaf from 09:30 to 12:30 h with the setting as follows: 400 μmol mol^{-1} CO_2, 300 μmol s^{-1} airflow, 30 °C leaf temperature and 1200 μmol mol^{-1} light intensity.

SPAD measurement. The SPAD value was measured in the blade of the fully grown uppermost leaf at the apical, middle, and basal parts using the SPAD-502 chlorophyll meter (Konica Minolta, Osaka, Japan) from 09:30 to 12:30 h.

Statistical analysis

Growth, physiological, and temperature data were analyzed for variance using SPSS version 28 (IBM, Armonk, New York, USA). The significance of variations among treatments was determined using Duncan's Multiple Range Test (DMRT) at $p < 0.05$. The Pearson's correlation and principal component analysis (PCA) were analyzed using R (R Foundation, New Zealand) with metan and FactoMineR packages, respectively (Lê et al., 2008).

RESULTS

Detecting temperature change through infrared thermography under salinity stress conditions

During the period of salt stress treatment, IR thermal images of 'Pokkali' seedlings were taken daily. An example of an IR thermal image 8 DAS was shown in Figure 1. Different temperatures, from high to low, were indicated with different color spectra of pale red to dark blue, respectively. According to Figure 1, the control group (leftmost pot) had more distribution of blue color around the canopy area than the salt stress groups. Most of the seedlings in salt stress groups were yellow in IR thermal image. After analyzing the leaf temperature with FLIR tools software, temperature change (ΔT) was calculated by subtracting $T_{salt\ stress}$ with $T_{control}$ ($T_{salt\ stress}$ - $T_{control}$). The results showed that there were nonsignificant differences in ΔT among groups during 1 to 3 DAS (Figure 2). At 4 to 8 DAS, seedlings treated with 160 mM NaCl had significantly higher ΔT than those in the 80 and 120 mM NaCl groups. The ΔT of all salt-treated groups kept rising until they reached the highest values at 8 DAS. The average leaf temperatures at 8 DAS of the control and the salt stress groups at 80, 120, and 160 mM NaCl were 31.99, 33.88, 35.03, and 37.20 °C, respectively. Therefore, ΔT of 80, 120, and 160 mM NaCl at 8 DAS were 1.89, 3.04, and 5.21 °C, respectively (Figure 2). Aside from temperature changes, the crop water stress index differences between control and salt stress groups (ΔCWSI; $CWSI_{salt\ stress}$ - $CWSI_{control}$) had no difference between salt stress groups during 0 to 3 DAS. Whereas the ΔCWSI of the 160 mM NaCl group during 4 to 8 DAS distinctly presented a significant maximum when compared with 80 and 120 mM groups (Figure 3A). Changes in the index of stomatal conductance (ΔI_G; $I_{Gsalt\ stress}$ - $I_{Gcontrol}$) showed an opposite trend with ΔT and ΔCWSI. The ΔI_G gradually decreased in 80, 120, and 160 mM NaCl groups in 4 DAS. The 160 mM NaCl group exhibited the reduction of ΔI_G at 5 DAS to 8 DAS. However, the ΔI_G of the 160 mM NaCl group showed a significant difference from the 80 and 120 mM NaCl groups (Figure 3B).

Figure 1. Infrared radiation (IR) thermal image (left) and visual image (right) of 'Pokkali' rice seedlings at 8 d after salt stress. The pictures were taken using the FILR C2 camera (FLIR Systems, Inc., USA). Seedlings in the buckets from left to right represented control, 80, 120, and 160 mM NaCl treatments, respectively.

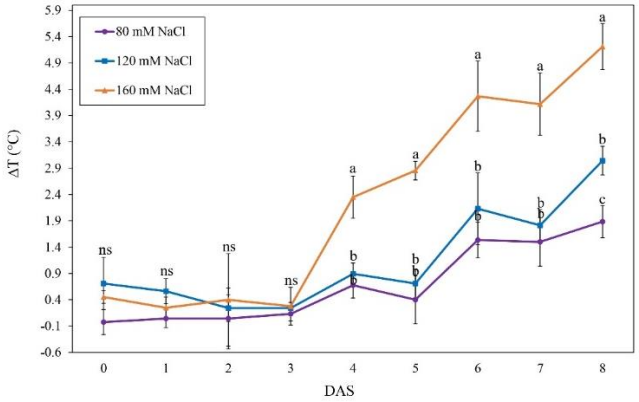

Figure 2. Effect of salt stress on temperature change (ΔT) in 'Pokkali' rice seedlings. The relationship between duration (day after stress, DAS) and ΔT (T_{stress} - $T_{control}$) was recorded from the day before salt stress application (0 DAS) to 8 DAS. The line with symbols ●, ■, ▲ represent ΔT of 80, 120, and 160 mM NaCl groups, respectively. Data were mean ± SEM of four replicates. Different letters indicated significant differences among NaCl groups in the same DAS by Duncan's Multiple Range Test at $p < 0.05$. ns: Nonsignificant.

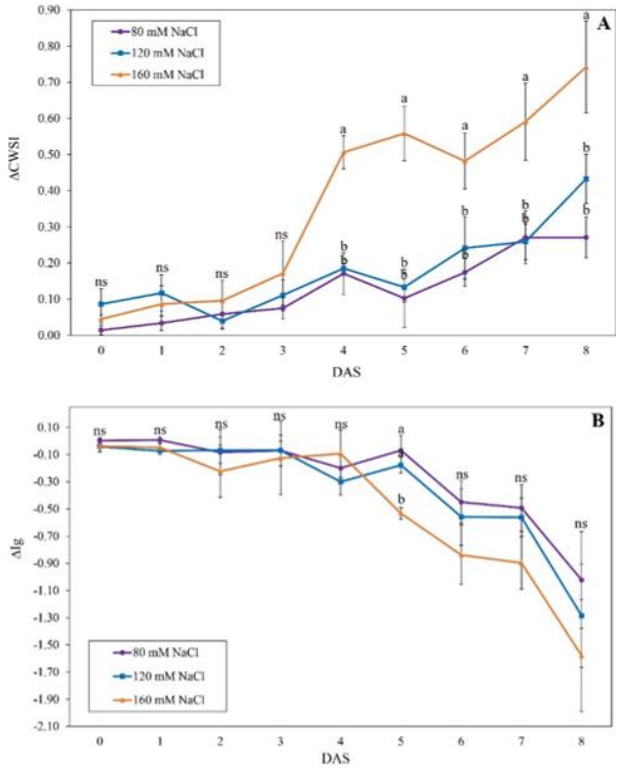

Figure 3. Effects of salt stress on changes in crop water stress index (Δ CWSI) (A) and index of stomatal conductance (ΔI_G) (B). ΔCWSI and ΔI_G were calculated by subtracting the number in the salt stress group from the number in the control group in the day before salt stress (0 day after stress, DAS) and during 1 to 8 DAS. The line with symbols ●, ■, ▲ represent ΔCWSI or ΔI_G of 80, 120, and 160 mM NaCl groups, respectively. Data were mean ± SEM of four replicates. Different letters indicated significant differences among NaCl groups in the same DAS by Duncan's Multiple Range Test at $p < 0.05$. ns: Nonsignificant.

Effect of salt stress on growth and physiological parameters

The growth parameters were investigated after salt-treatment for 8 d and are shown in Table 1. At 8 DAS, we observed lower reductions in shoot fresh weight at 80, 120, and 160 mM NaCl: 6.75%, 36.57%, and 34.36%, respectively. Similarly, reductions in root fresh weights at 80, 120, and 160 mM NaCl were 19.27%, 37.93%, and 35.07%. Seedlings exposed to 120 and 160 mM NaCl had slightly lower shoot dry weight than those in the control group. The root dry weight of seedlings seemed to reduce with increasing NaCl concentrations. However, the values were nonsignificant among the groups. The results indicated that NaCl had slight effects on shoot and root growth as shown by nonsignificant difference data in Table 1. Seedlings subjected to 0, 80, 120, and 160 mM NaCl showed nonsignificant differences in root length. However, shoot length exhibited the highest reduction percentage at 120 mM NaCl (10.72%). These results suggest that the control group had no significant differences compared to the 80 and 160 mM NaCl groups, while the 120 mM NaCl group had a significant effect on shoot length. Along with these, seedlings in the control group exhibited the highest RWC (97.53 ± 0.01%). The reduction in salt stress groups was 5.96%, 3.42%, and 3.52% at 80, 120, and 160 mM NaCl, respectively. Similarly, RWC did not differ significantly among groups (Table 1). Surprisingly, NaCl showed significant effects on some physiological responses of 'Pokkali' seedlings (Figure 4). Seedlings subjected to salt stress showed signs of membrane damage which was indicated by the significant increases in EL (Figure 4A) and MDA content (Figure 4B). The NaCl at 160 mM caused the highest percentage of EL. Meanwhile, the MDA content of seedlings at 120 mM NaCl (25.19 ± 1.23 nmol g^{-1} FW) and 160 mM (25.49 ± 3.37 nmol g^{-1} FW) were higher than control and 80 mM NaCl. However, the SPAD values at 80 and 120 mM NaCl (40.48 ± 1.18, 40.54 ± 0.90, respectively) were the highest values among salt-tested groups (Figure 4C). In addition, salt stress conditions also affected the leaf gas exchange of seedlings (Figure 4D-4F). The P_n and T_r of the control group differed significantly with the salt stress conditions (Figure 4D and Figure 4E). The P_n of seedlings in 120 mM NaCl and 160 mM NaCl sharply dropped from the control group, with reduction percentages of 65.76% and 70.99%, respectively. A similar change was observed in the T_r. The g_s of the control group and the salt stress groups were significantly different (Figure 4F). Seedlings exposed to 80, 120, and 160 mM NaCl exhibited very low g_s with reduction percentages of 75.35%, 86.59% and 92.78%, respectively.

Table 1. Effect of various NaCl concentrations on fresh weight, dry weight, shoot length, root length, and relative water content of 'Pokkali' rice seedlings at 8 d after stress. Data were mean ± SEM of four replicates. Different letters indicated significant differences among NaCl concentrations by Duncan's multiple range test at $p < 0.05$.

NaCl concentrations	Fresh weight		Dry weight		Shoot length	Root length	Relative water content
	Shoot	Root	Shoot	Root			
mM	g plant^{-1}		g plant^{-1}		cm		%
Control	16.05 ± 1.68^{a}	6.55 ± 0.60^{a}	2.16 ± 0.91^{a}	0.82 ± 0.09^{a}	71.64 ± 2.00^{ab}	14.66 ± 0.19^{a}	97.53 ± 0.01^{a}
80	14.97 ± 2.12^{a}	5.28 ± 1.11^{a}	2.27 ± 1.45^{a}	0.60 ± 0.12^{a}	73.65 ± 1.45^{a}	18.59 ± 2.26^{a}	91.71 ± 0.03^{a}
120	10.18 ± 1.46^{a}	4.06 ± 0.82^{a}	1.88 ± 0.84^{a}	0.44 ± 0.08^{a}	63.96 ± 1.93^{c}	14.13 ± 0.41^{a}	94.18 ± 0.01^{a}
160	10.53 ± 1.52^{a}	4.25 ± 0.98^{a}	2.08 ± 0.64^{a}	0.42 ± 0.08^{a}	67.67 ± 1.16^{bc}	15.45 ± 0.18^{a}	94.09 ± 0.01^{a}

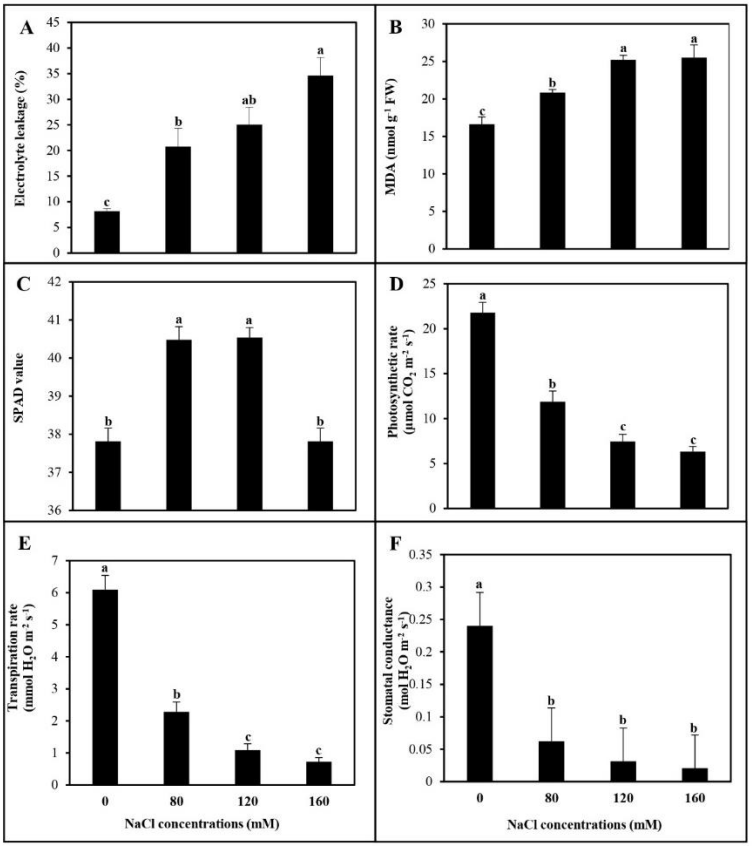

Figure 4. Effect of salt stress on electrolyte leakage (A), malondialdehyde content (MDA) (B), SPAD value (C), photosynthetic rate (D), transpiration rate (E), and stomatal conductance (F) of 'Pokkali' rice seedlings at 8 d after stress. Bars represented the mean ± SEM of four replicates. Different letters indicated significant differences among NaCl concentrations by Duncan's Multiple Range Test at $p < 0.05$.

Correlation among thermal, growth, and physiological parameters

Spectacularly, the correlation analysis using R with the package metan showed the positive and negative relationships among the related-IR thermography, physiological, and growth parameters on 26 d 'Pokkali' rice seedlings after NaCl-treated for 8 d. According to Figure 5, the correlation coefficients (r) between +1 and -1 were denoted with various colors ranging from dark blue to pale red. The correlated matrix as shown in Figure 5 exhibited that leaf temperature (Temp) had negative relationships with the leaf gas exchange parameters, including T_r ($r = -0.580$, $p < 0.05$), P_n ($r = -0.553$, $p < 0.05$), and g_s ($r = -0.600$, $p < 0.05$). Additionally, the Temp was negatively related to some growth parameters, such as SFW ($r = -0.530$, $p < 0.05$), RFW ($r = -0.638$, $p < 0.01$), and RDW ($r = -0.676$ $p < 0.01$). Against, EL and MDA revealed positive relationships with Temp at $r = 0.429$ and $r = 0.543$ at $p < 0.05$, respectively. Also, the CWSI had strong negative relationships with T_r ($r = -0.800$, $p < 0.01$), P_n ($r = -0.799$, $p < 0.01$), and g_s ($r = -0.754$, $p < 0.01$). Surprisingly, I_G had strongly positive relationships with T_r ($r = 0.788$, $p < 0.01$), P_n ($r = 0.787$, $p < 0.01$), and g_s ($r = -0.754$, $p < 0.01$). On the other hand, I_G was negatively correlated with EL ($r = -0.719$, $p < 0.01$) and MDA ($r = -0.803$, $p < 0.01$). Moreover, this study clearly showed that Temp had a strongly significant positive and negative relationship with CWSI ($r = 0.726$, at $p < 0.01$) and I_G ($r = -0.694$, at $p < 0.01$), respectively. Besides, significantly negative correlations were observed among leaf gas exchange indices, EL and MDA.

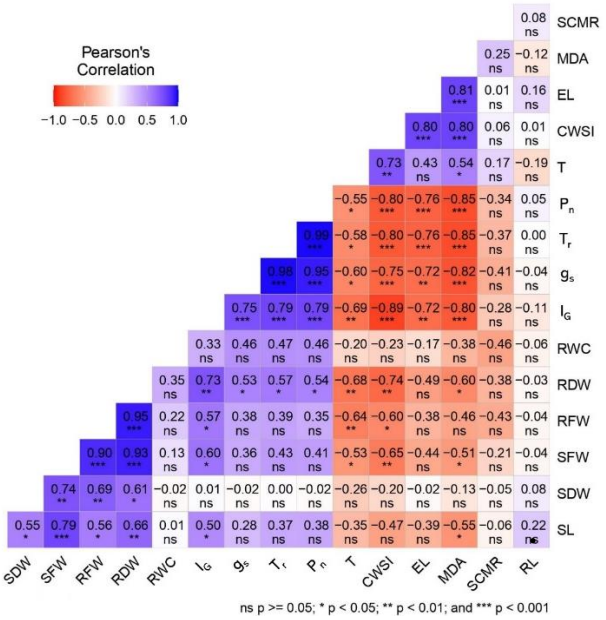

Figure 5. The heat map correlation matrix generated using the metan package in R shows correlation among 15 thermal, growth, biochemical, and physiological parameters investigated in 26-d-old 'Pokkali' rice seedlings after being salt-treated for 8 d. Their correlated levels were represented with a dark blue (strong positive relationship) to pale red (strong negative relationship). Each cell in the correlation matrix is represented by a Pearson's correlation coefficient (r). *, **, and ***: Significant differences between their relationships by Pearson's correlation at $p < 0.05$, $p < 0.01$, and $p < 0.001$, respectively. SDW: shoot dry weight; SFW: shoot fresh weight; RFW: root fresh weight; RDW: root dry weight; RWC: relative water content; I_G: index of stomatal conductance; g_S: stomatal conductance; Tr transpiration rate; P_n: photosynthetic rate; T: leaf temperature; CWSI: crop water stress index; EL: electrolyte leakage; MDA: malondialdehyde content; SCMR: SPAD chlorophyll meter reading; RL: root length; SL: shoot length.

Principal component analysis

Fifteen IR-thermal, growth, and physiological variables were subjected to PCA in order to minimize the dimensionality of the data and find potential correlations between the observed characteristics in all treatments. The individual PCA in Figure 6 revealed that PC1 and PC2 accounted for 52.7% and 16.4% of the variance, respectively, with a cumulative percentage of 69.1%. In the PC1 dimension, the data points were divided into four distinct groups, comprising the control group, 80 mM NaCl group, 120 mM NaCl group, and 160 mM NaCl group. Interestingly, the salt-treated groups in the 80, 120, and 160 mM NaCl groups exhibited close grouping and were positioned toward the left side, while the control group was positioned on the right side. Furthermore, the variables that contributed to the grouping in Figure 6 were presented in Figure 7, where it can be observed that the growth parameters, including RDW, SDW, SFW, RFW, SL, and RL, were grouped on the right upper side of the plot. Conversely, the biochemical parameters, such as EL and MDA, were clustered with SCMR and CWSI. Notably, the variable Temp, obtained through IR-thermography, was situated on the left lower side of the plot, while I_G was closely associated with the leaf gas exchange parameters (T_r, P_n, and g_s) as well as RWC on the right lower side. Moreover, the growth parameters exhibited a clear positive relationship in the PCA biplots, while Temp displayed a distinctly negative relationship. Additionally, the top 10 highest-contributing traits in PC1 were CWSI, I_G, T_r, MDA, RDW, P_n, g_s, EL, SFW, and RFW, whereas PC2 demonstrated the SDW, SFW, RFW, SL, g_s, P_n, RDW, T_r, RWC, and EL.

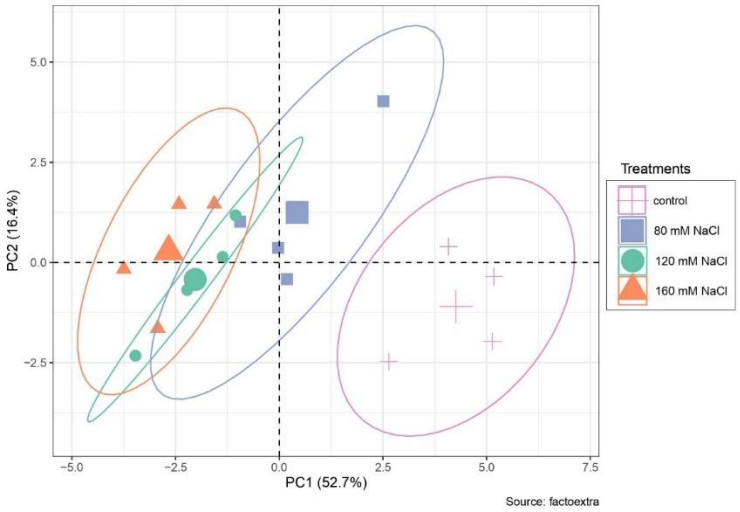

Figure 6. The individual factor map analyzed using FactoMineR package in R of control, 80, 120, and 160 mM NaCl groups in 26-d-old 'Pokkali' rice seedlings after being salt-treated for 8 d. The purple, blue, red, and green circles represented the data dispersion of control, 80, 120, and 160 mM NaCl groups, respectively. The plus, square, circle, and triangle symbols were individual replicates from control, 80, 120, and 160 mM NaCl groups, respectively.

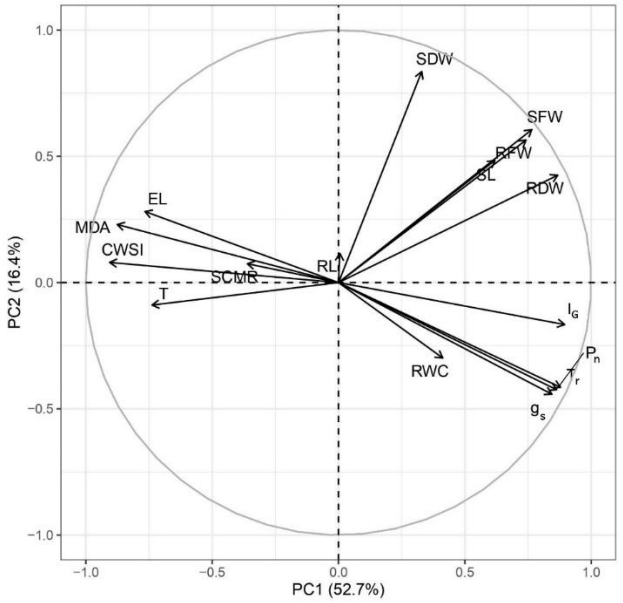

Figure 7. Principal component analysis (PCA) of 15 thermal, growth, biochemical, and physiological parameters investigated in 26-d-old 'Pokkali' rice seedlings after being salt-treated for 8 d. The PCA was analyzed using FactoMineR package in R. Arrows refer the powerful strength of the trait impact on the first two components in plot. P_n: Photosynthetic rate; g_s: stomatal conductance; T_r: transpiration rate; EL: electrolyte leakage; MDA: malondialdehyde content; SL: shoot length; RL: root length; SFW: shoot fresh weight; SDW: shoot dry weight; RFW: root fresh weight; RDW: root dry weight; SCMR: SPAD chlorophyll meter reading; T: leaf temperature; CWSI: crop water stress index; I_G: index of stomatal conductance.

DISCUSSION

The IR-thermography has been employed to detect the infrared radiation emitted by objects with wavelengths typically falling within the range of 700 nm to 1000 µm (Tsai and Hamblin, 2017). Furthermore, it has been explored in the context of studying salt stress responses in cereal crops. Salt stress induces more emission of infrared radiation in plants, primarily due to water deficiency (Kwon et al., 2015). This condition arises from physiological reactions associated with osmotic stress, which in turn trigger stomatal closure in plants (Munns and Tester, 2008). Subsequent stomatal closure results in diminished transpiration, leading to the accumulation of heat energy within the plant. This leads to increased leaf temperatures (Orzechowska et al., 2021) owing to the significant energy consumption during the transition of water molecules from liquid to vapor state (Jones et al., 2009). The results from our study showed that salt stress could affect temperature changes (ΔT) in 'Pokkali' rice seedlings, and these changes could be detected by FLIR C2 portable thermal camera. Seedlings in salt-treated groups initially received 40 mM NaCl for three days during the period of salinity exposure. Therefore, their ΔT exhibited similar trends and were lower than 1 °C. The rapid increase of ΔT was found when 'Pokkali' rice seedlings were subjected to 160 mM NaCl during 4 to 8 DAS. Increasing ΔT was also observed in 80 and 120 mM NaCl groups, but with significantly lower magnitude. Moreover, changes in crop water stress index (ΔCWSI) depicted similar results with ΔT. In the study by Pradawet et al. (2022), it was found that CWSI could effectively serve as an indicator for detecting water stress in maize, exhibiting a robust negative correlation with g_s. Our own study corroborates these observations by revealing robust associations between ΔCWSI and the leaf gas exchange parameters illustrated in Figure 5. These findings suggest that ΔCWSI may serve as a reliable indicator of water stress in cereal crops. The distinction in ΔI_G among the salt-treated groups was first observed at 5 DAS. Notably, nonsignificant differences in ΔI_G were detected among the groups for the remainder of the salt treatment period. However, ΔI_G was appeared to consistent with P_n, T_r, and g_s.

'Pokkali', a rice landrace, has been widely used for comparative physiological research, allele mining, and the discovery of molecular markers linked to salinity tolerance (Mishra et al., 2021). Our findings revealed that 'Pokkali' seedlings exposed to 80 to 160 mM NaCl showed low stomatal conductance, which resulted in greatly reduced transpiration and photosynthesis. The increment of leaf greenness was recorded, and this change may be due to the adaptation to osmotic stress by curling the leaves. Leaf curling decreases leaf width and can increase the density of chloroplast, which results in a higher SPAD value (Tran et al., 2017). Apart from this, it was exhibited that the SPAD values of the control group and 160 mM NaCl group had nonsignificant difference. Despite that, seedlings in the 160 mM NaCl group had a decrease in leaf width compared to the control. Concurrently, the 160 mM NaCl was high enough to ruin the structure and functions of chloroplasts which resulted in the reduction of SPAD readings. Moreover, we observed increases in cell damage indicators, including MDA content and electrolyte leakage, in salt-stressed seedlings. The augmentations of cell damage parameters are again caused by stomatal closure which limits the concentration of the leaf CO_2 contributing to the passing of electrons from electron transport systems to O_2 which creates reactive oxygen species (ROS) (Amirjani, 2010). These ROS can react with membrane lipids by lipid peroxidation leading to the production of MDA and membrane damage (Ludwiczak et al., 2021). Interestingly, our results reveal that a low concentration of 80 mM NaCl had a minor impact on most physiological and growth traits, while it did promote an increase in both shoot and root lengths. Various physiological and growth parameters, such as electrolyte leakage, malondialdehyde content, SPAD readings, photosynthetic rate, and transpiration rate, in seedlings exposed to 80 mM NaCl were less affected when compared to those exposed to 120 and 160 mM NaCl. Notably, both shoot and root lengths exhibited a significant increase when compared to the control group. Kumar et al. (2017) observed that even low stress concentrations trigger the production of ROS, which in turn function as signaling molecules for stress tolerance. The accumulation of ROS below the stress threshold activates various processes in plants, including growth, development, and adaptation, through interactions with phytohormones like auxin, abscisic acid, and gibberellin (Saini et al., 2018). Furthermore, ROS plays a role in stimulating MAPK cascades, which govern auxin signaling at the upstream level (Jagodzik et al., 2018). This signaling cascade leads to enhanced shoot growth in the presence of salinity stress. Additionally, the previous study by Ma et al. (2012) found that ROS

generated by NADPH oxidases serve as signal molecules and positive transducers that modulate the Na^+/K^+ balance in plants under salt stress.

Concurrently, some growth parameters displayed a slightly consistent response to the IR-thermal indices and physiological performances. In this study, our research exhibited that adding 80 to 160 mM NaCl to the nutrient solution for eight days slightly affected fresh and dry mass accumulations of the 26-d-old 'Pokkali' rice seedlings, notably 120 and 160 mM NaCl group, even though there was nonsignificant difference among groups. The RWC of control and salt-treated seedlings did not significantly differ. These results were consistent with Pamuta et al. (2022), who found that the RGD4 line, which is the salt-tolerant recombinant inbred line (RIL), had lower reduction percentages of shoot and root weight, as well as RWC, than other jasmine rice cultivars or lines under salt-treated conditions. Surprisingly, this salt-tolerant rice cultivar still maintained its biomass throughout the experimental period, even though the photosynthetic rate in salt-treated groups, especially 120 and 160 mM NaCl groups, was fourfold less than the control group. Predominantly, the slight reductions in mass accumulation and RWC under salt stress can be caused by osmotic and ionic stresses. Firstly, osmotic stress instantly occurs due to the different water potential around their rhizosphere, leading to reductions in shoot growth and leaf expansion (Munns and Tester, 2008). Moreover, it also contributes to the water deficit, which stimulates the activity of the abscisic acid (ABA), bringing about stomatal closure (Kumar et al., 2013). The ABA reception stimulates the formation of ROS, resulting in stomatal closure, which can cause limitations in gas exchange, transpiration, and photosynthesis (Ye et al., 2012; Liu et al., 2022). Secondly, the ionic stress resulting from ion transportation and ion accumulation can impair cellular machinery, including quantum yield of photosystem II (PSII) and photosystem I (PSI), contributing to disrupting photosynthesis and inducing a slight decrease in mass accumulation (Soda et al., 2018). Importantly, 'Pokkali' serves as a standard for salt tolerance, which has a quantitative trait locus (QTL) that regulates the balance of the ratio between Na^+ and K^+ (Bonilla et al., 2002; Soda et al., 2013). Moreover, the results from the comparative physiological and biochemical study between salt-tolerant 'Pokkali' and salt-susceptible IR64 seedlings under high salt conditions by Mishra et al. (2021) indicated that the ability of 'Pokkali' seedlings to tolerate salinity by maintaining their growth is a result of the harmonious interplay of numerous physiological and biochemical factors. These factors encompass maintaining cellular balance in terms of ions, facilitating electron transport, optimizing PSII, ensuring efficient photosynthesis, activating adaptive defense mechanisms, accumulating osmolytes, preserving membrane integrity, and creating an ideal biochemical environment within the cells. As a result, their growth was not profoundly or significantly affected by salt stress.

Although the growth performance of 'Pokkali' rice in our study was not profoundly affected by salt stress, the analysis of datasets with IR-thermal and physiological variables using PCA showed the separation of control and salt-treated group. In the earlier research conducted by Shunkao et al. (2022), they investigated how three different wheat cultivars responded to various types of stress: Heat stress, salinity stress, and a combination of salt and heat stress. They used PCA to analyze the data, and their findings revealed that the growth and physiological characteristics of the wheat cultivars could be categorized into two distinct groups. The first group included those subjected to salt stress and the combination of salt and heat stress, while the second group consisted of the control group and those exposed to heat stress alone. Our PCA results also showed that the PC1, which explained 52.5% of the total variability among traits or individuals, was mostly associated with CWSI and I_G. These findings demonstrate the advantages of employing IR thermography for investigating the response to salt stress. This is due to its non-invasive methodology and its ability to provide extensive data for multidimensional analysis, which holds potential for future screening of different rice genotypes for salt tolerance.

CONCLUSIONS

Infrared radiation (IR) thermal imaging has been used for studying plant response under unfavorable conditions such as salt stress by detecting canopy temperature change. This study shows that salt stress conditions affect physiological responses such as membrane stability, stomatal conductance, transpiration, and photosynthesis, leading to canopy temperature changes in 'Pokkali' rice. Although the 'Pokkali' rice

has been classified as a salt-tolerant cultivar, IR thermography can detect the osmotic stress response of this rice. Besides, changes in temperature and crop water stress index can indicate the osmotic stress with different NaCl concentrations. Due to the non-destructive nature of IR thermography, it can be used to monitor temperature changes in rice seedlings during a saline-treated period. Moreover, this approach will be applied to monitor the difference in responses among various rice cultivars in the future.

Author contribution

Conceptualization: W.L., C.P., N.K., P.T. Methodology: W.L., C.P. Investigation: C.P. Writing-original draft: C.P. Writing-review & editing: P.T., W.L., N.K. Supervision: P.T. Project administration: W.L. Funding acquisition: P.T., W.L., N.K. All co-authors reviewed the final version and approved the manuscript before submission.

Acknowledgements

Financial support was made available for this research by 1) the National Research Council of Thailand (NRCT) through the Senior Research Scholar Project of Prof. Dr. Piyada Theerakulpisut (Project No. NRCT813/2563), and 2) Division for Research and Graduate Studies, Khon Kaen University under the Research Program RP66-1-003. 'Pokkali' rice seeds were kindly provided by Salt-Tolerant Rice Research Group, Faculty of Science, Khon Kaen University. The authors would like to thank Supranee Santanoo, Wongsakorn Wongla, and Jittree Sawangwong for their technical assistance.

References

Amirjani, M.R. 2010. Effect of NaCl on some physiological parameters of rice. European Journal of Biological Science 3:6-16.

Bayoumi, T., El-Hendawy, S., Yousef, M., Emam, M., Okasha, S. 2014. Application of infrared thermal imagery for monitoring salt tolerant of wheat genotypes. Journal of American Science 11(23):227-234. doi:10.3390/plants11233269.

Bonilla, P., Dvorak, J., Mackill, D., Deal, K., Gregorio, G. 2002. RLFP and SSLP mapping of salinity tolerance genes in chromosome 1 of rice (*Oryza sativa* L.) using recombinant inbred lines. Philippine Agricultural Scientist 85:68-76.

Chen, T., Zhu, Y., Chen, K., Shen, C., Zhao, X., Shabala, S., et al. 2019. Identification of new QTL for salt tolerance from rice variety Pokkali. Journal of Agronomy and Crop Science 206:202-213. doi:10.1111/jac.12387.

FAO. 2022. Global map of salt-affected soils. FAO SOILS PORTAL. Food and Agriculture Organization of the United Nations. Available at https://www.fao.org/soils-portal/data-hub/soil-maps-and-databases/global-map-of-salt-affected-soils/en/ (accessed 31 July 2023).

Filek, M., Walas, S., Mrowiec, H., Rudolphy-Skórska, E., Sieprawska, A., Biesaga-Kos´cielniak, J. 2012. Membrane permeability and micro- and macroelement accumulation in spring wheat cultivars during the short-term effect of salinity- and PEG-induced water stress. Acta Physiologiae Plantarum 34(3):985-995. doi:10.1007/s11738-011-0895-5.

Heath, R.L., Packer, L. 1968. Photoperoxidation in isolated chloroplasts: I. Kinetics and stoichiometry of fatty acid peroxidation. Archives of Biochemistry and Biophysics 125(1):189-198. doi:10.1016/0003-9861(68)90654-1.

Jagodzik, P., Tajdel-Zielinska, M., Ciesla, A., Marczak, M., Ludwikow, A. 2018. Mitogen-activated protein kinase cascades in plant hormone signaling. Frontiers in Plant Science 9:1-26. doi:10.3389/fpls.2018.01387.

James, R.A., Sirault, X.R.R. 2012. Infrared thermography in plant phenotyping for salinity tolerance. Methods in Molecular Biology 913:173-189. doi:10.1007/978-1-61779-986-0_11.

Jones, H.G. 1999. Use of infrared thermometry for estimation of stomatal conductance as a possible aid to irrigation scheduling. Agricultural and Forest Meteorology 95(3):139-149. doi:10.1016/S0168-1923(99)00030-1.

Jones, H., Serraj, R., Loveys, B., Xiong, L., Wheaton, A., Price, A.H. 2009. Thermal infrared imaging of crop canopies for remote diagnosis and quantification of plant responses to water stress in the field. Functional Plant Biology 36:978-989. doi:10.1071/FP09123.

Kumar, V., Khare, T., Sharma, M., Wani, S.H. 2017. ROS-induced signaling and gene expression in crops under salinity stress. p. 159-184. In Khan, M., Khan, N. (eds.). Reactive oxygen species and antioxidant systems in plants: Role and regulation under abiotic stress. Springer, Singapore.

Kumar, K., Kumar, M., Kim, S.-R., Ryu, H., Cho, Y.-G. 2013. Insights into genomics of salt stress response in rice. Rice 6(1):27. doi:10.1186/1939-8433-6-27.

Kwon, T., Kim, K., Yoon, H.J., Lee, S., Kim, B., Siddiqui, Z.S. 2015. Phenotyping of plants for drought and salt tolerance using infra-red thermography. Plant Breeding and Biotechnology 3:299-307. doi:10.9787/PBB.2015.3.4.299.

Lê, S., Josse, J., Husson, F. 2008. FactoMineR: An R Package for Multivariate Analysis. Journal of Statistical Software 25:1-18. doi:10.18637/jss.v025.i01.
Liu, C., Mao, B., Yuan, D., Chu, C., Duan, M. 2022. Salt tolerance in rice: Physiological responses and molecular mechanisms. The Crop Journal 10(1):13-25. doi:10.1016/j.cj.2021.02.010.
Ludwiczak, A., Osiak, M., Pérez, S., Lubińska-Mielińska, S., Piernik, A. 2021. Osmotic stress or ionic composition: Which affects the early growth of crop species more? Agronomy 11:1-15. doi:10.3390/agronomy11030435.
Ma, L., Zhang, H., Sun, L., Jiao, Y., Zhang, G., Miao, C., et al. 2012. NADPH oxidase AtrbohD and AtrbohF function in ROS-dependent regulation of Na^+/K^+ homeostasis in *Arabidopsis* under salt stress. Journal of Experimental Botany 63(1):305-317. doi:10.1093/jxb/err280.
Mishra, M., Wungrampha, S., Kumar, G., Singla-Pareek, S.L., Pareek, A. 2021. How do rice seedlings of landrace Pokkali survive in saline fields after transplantation? Physiology, biochemistry, and photosynthesis. Photosynthesis Research 150(1):117-135. doi:10.1007/s11120-020-00771-6.
Munns, R., Tester, M. 2008. Mechanisms of salinity tolerance. Annual Review of Plant Biology 59(1):651-681. doi:10.1146/annurev.arplant.59.032607.092911.
Orzechowska, A., Trtílek, M., Tokarz, K.M., Szymańska, R., Niewiadomska, E., et al. 2021. Thermal analysis of stomatal response under salinity and high light. International Journal of Molecular Sciences 22(9):1-15. doi:10.3390/ijms22094663.
Pamuta, D., Siangliw, M., Sanitchon, J., Pengrat, J., Siangliw, J., et al. 2022. Physio-biochemical traits in improved "KDML105" jasmine rice lines containing drought and salt tolerance gene under drought and salt stress. Chilean Journal of Agricultural Research 82:97-110. doi:10.4067/S0718-58392022000100097.
Pradawet, C., Khongdee, N., Pansak, W., Spreer, W., Hilger, T., Cadisch, G. 2022. Thermal imaging for assessment of maize water stress and yield prediction under drought conditions. Journal of Agronomy and Crop Science 209:1-15. doi:10.1111/jac.12582.
Shunkao, S., Thitisaksakul, M., Pongdontri, P., Theerakulpisut, P. 2022. Additive effects of combined heat and salt stress is manifested in an enhanced sodium ions accumulation and increased membrane damage in wheat seedlings. Chilean Journal of Agricultural Research 82:552-563. doi:10.4067/S0718-58392022000400552.
Saini, P., Gani, M., Kaur, J.J., Chand, L., Singh, C., Chauhan, S.S., et al. 2018. Reactive oxygen species (ROS): A way to stress survival in plants. p. 127-153. In Zargar, S., Zargar, M. (eds.) Abiotic stress-mediated sensing and signaling in plants: An omics perspective. Springer, Singapore. doi:10.1007/978-981-10-7479-0_4.
Siddiqui, Z.S., Cho, J.I., Park, S.H., Kwon, T.R., Ahn, B.O., Lee, G.S., et al. 2014. Phenotyping of rice in salt stress environment using high-throughput infrared imaging. Acta Botanica Croatica 73:149-158. doi:10.2478/botcro-2013-0027.
Sirault, X.R.R., James, R.A., Furbank, R.T. 2009. A new screening method for osmotic component of salinity tolerance in cereals using infrared thermography. Functional Plant Biology 36(11):970-977. doi:10.1071/FP09182.
Soda, N., Gupta, B.K., Anwar, K., Sharan, A., Govindjee, Singla-Pareek, S.L., et al. 2018. Rice intermediate filament, OsIF, stabilizes photosynthetic machinery and yield under salinity and heat stress. Scientific Reports 8(1):4072. doi:10.1038/s41598-018-22131-0.
Soda, N., Kushwaha, H.R., Soni, P., Singla-Pareek, S.L., Pareek, A. 2013. A suite of new genes defining salinity stress tolerance in seedlings of contrasting rice genotypes. Functional and Integrative Genomics 13(3):351-365. doi:10.1007/s10142-013-0328-1.
Tran, S., Nhi, P., Trinh, S. 2017. Salinity effect at seedling and flowering stages of some rice lines and varieties (*Oryza sativa* L.) Journal of Agricultural Science and Technology A 7:32-39. doi:10.17265/2161-6256/2017.10.005S.
Tsai, S.-R., Hamblin, M.R. 2017. Biological effects and medical applications of infrared radiation. Journal of Photochemistry and Photobiology B 170:197-207. doi:10.1016/j.jphotobiol.2017.04.014.
Weatherly, P.E. 1951. Studies of the water relations of the cotton plant II diurnal and seasonal variations in relative turgidity and environmental factors. New Phytologist 50(1):36-51.
Ye, N., Jia, L., Zhang, J. 2012. ABA signal in rice under stress conditions. Rice 5(1):1-9. doi:10.1186/1939-8433-5-1.
Yoshida, S., Fomo, D.A., Cock, J.H., Gomez, K.A. 1976. Laboratory manual for physiological studies of rice. International Rice Research Institute, Los Baños, Philippines.